International Journal of Trend in Scientific Research and Development (IJTSRD)
Volume 10 Issue 3, May-Jun 2026 Available Online: www.ijtsrd.com e-ISSN: 2456 – 6470

Wireless Sensor Network-Based Real-Time Underground Water Lead (Pb), Cadmium (Cd) and Chromium (Cr) Concentrate Monitoring and Prediction in Warri City, Niger Delta: A Smart Environmental Management Approach

Odesa Ogaga Edward, Ugbeh Raymond Nduka, Obonyano Kingdom, Idama Omokaro

Department of Computer Engineering, Southern Delta University, Ozoro, Delta, Nigeria

ABSTRACT

The Niger Delta region, particularly Warri City, faces critical groundwater contamination resulting from petroleum exploration, industrial discharges, urbanization, and inadequate waste management practices. This study presents a Wireless Sensor Network (WSN)-based framework that integrates Internet of Things (IoT) sensors, cloud computing, machine learning, and geospatial analysis for real-time monitoring and prediction of groundwater pollutants. Forty-five sensor nodes were deployed across industrial, residential, agricultural, and wetland zones of Warri City, continuously monitoring physicochemical parameters, petroleum hydrocarbons, and heavy metals including lead (Pb), cadmium (Cd), chromium (Cr), and nickel (Ni) over an 18-month period. Predictive models comprising Random Forest (RF), Support Vector Regression (SVR), and Long Short-Term Memory (LSTM) networks were developed to forecast contamination trends. The WSN framework demonstrated high data transmission reliability and robust spatial hazard mapping capabilities. Results revealed elevated concentrations of Pb and Cd that exceeded World Health Organization (WHO) drinking water guidelines in several monitoring locations. While nickel contamination was detected, elevated concentrations were highly localized within industrial areas, remaining at safe baseline levels within residential zones. Total Petroleum Hydrocarbon (TPH) concentrations exhibited significant seasonal variation, reaching levels far above recommended environmental thresholds during the dry season. Among the predictive models evaluated, LSTM demonstrated superior forecasting performance with an R2 value of 0.91. Human health-risk assessment showed Hazard Index (HI) values exceeding safe limits across all population groups, with infants (HI=5.67) and pregnant women (HI=4.01) identified as the most vulnerable demographics. The findings underscore the severity of groundwater contamination in Warri City and demonstrate the potential of IoT-enabled WSN systems for continuous environmental monitoring, predictive analytics, and evidence-based groundwater management in the Niger Delta and similar industrialized regions.

How to cite this paper: Odesa Ogaga Edward | Ugbeh Raymond Nduka | Obonyano Kingdom | Idama Omokaro "Wireless Sensor Network-Based Real-Time Underground Water Lead (Pb), Cadmium (Cd) and Chromium (Cr) Concentrate Monitoring and Prediction in Warri City, Niger Delta: A Smart Environmental Management Approach" Published in International Journal of Trend in Scientific Research and Development (ijtsrd), ISSN: 2456-6470, Volume-10 | Issue-3, June 2026, pp.740-751, URL: www.ijtsrd.com/papers/ijtsrd133292.pdf

IJTSRD133292

KEYWORDS: *Wireless Sensor Networks (WSN); Internet of Things (IoT); Groundwater Quality Monitoring; Heavy Metals; Lead (Pb); Cadmium (Cd); Chromium (Cr); Nickel (Ni); Total Petroleum Hydrocarbons (TPH); Machine Learning; Long Short-Term Memory (LSTM); Health Risk Assessment; Niger Delta; Warri City; Predictive Analytics.*

INTRODUCTION

Underground water contamination in Warri City represents a growing ecological and public health challenge within the Niger Delta region of Nigeria. Rapid industrialization, petroleum refining activities, urban expansion, and inadequate waste management practices have contributed to the degradation of groundwater resources, resulting in elevated concentrations of heavy metals and petroleum hydrocarbons in aquifer systems. Among the most concerning contaminants are lead (Pb), cadmium (Cd), chromium (Cr), and nickel (Ni), which are frequently associated with industrial effluents, refinery operations, and anthropogenic activities. These contaminants pose significant risks to human health due to their persistence, bioaccumulation potential, and toxicity [1], [2].

Conventional groundwater monitoring approaches based on periodic field sampling and laboratory analysis are often expensive, time-consuming, and inadequate for capturing the temporal and spatial variability of contamination events. Consequently, there is an increasing need for intelligent monitoring systems capable of providing continuous, real-time information on groundwater quality. Recent advances in the Internet of Things (IoT), Wireless Sensor Networks (WSNs), cloud computing, and machine learning technologies have enabled the development of cost-effective environmental monitoring platforms that support real-time data acquisition, predictive analytics, and evidence-based decision-making [3], [4].

Wireless Sensor Networks offer significant advantages for environmental monitoring through distributed sensing, low-power communication, and automated data transmission. When integrated with cloud-based analytics and machine learning algorithms, WSNs can facilitate early detection of contamination events, prediction of pollutant trends, and rapid dissemination of alerts to environmental managers and public health agencies. Furthermore, combining geospatial analysis with predictive modeling provides a robust framework for identifying contamination hotspots and assessing potential risks to exposed populations.

Therefore, this study proposes a Wireless Sensor Network-based real-time monitoring framework for underground water quality assessment in Warri City. The framework integrates IoT-enabled sensors, LoRaWAN communication technology, cloud-based data processing, machine learning algorithms, and health-risk assessment models to support sustainable groundwater management. Specifically, the objectives of this study are to: (i) deploy a comprehensive WSN for real-time groundwater quality monitoring; (ii) characterize the spatio-temporal distribution of Pb, Cd, Cr, Ni, and petroleum hydrocarbon contaminants; (iii) develop machine learning models for pollutant prediction and forecasting; and (iv) evaluate potential human health risks associated with long-term exposure to contaminated groundwater.

LITERATURE REVIEW

A. Underground Water Contamination in the Niger Delta

The Niger Delta faces significant underground water contamination due to industrial, oil exploration, and waste management practices. Chowdury et al. [5] and Anynanwu et al [6] highlight that the region's shallow aquifers are especially vulnerable to pollutants such as petroleum hydrocarbons, heavy metals, and industrial effluents. These pollutants often exceed WHO limits, posing serious environmental and health risks. Alam et al. [7] and B. Guo et al. [8] emphasize that heavy metals like lead (Pb), cadmium (Cd), and chromium (Cr) are common contaminants, with industrial zones suffering the highest concentrations.

B. Heavy Metal Contamination and Health Risks

Heavy metals are a critical concern due to their persistence in the environment and toxicity. Pb, Cd, and Cr contaminate the region's groundwater primarily due to oil extraction activities. Anyanwu et al. [6] and Emoyan et al [9] observed that Pb concentrations in Warri City far exceed safe limits, contributing to neurological damage, especially in children. Cadmium is a carcinogen linked to kidney damage, while Chromium (Cr VI) causes respiratory issues and organ damage. Bawa-Allah et al. [10]noted that vulnerable groups, including infants and pregnant women, face heightened health risks from prolonged exposure.

C. Petroleum Hydrocarbon Contamination

TPH contamination, arising from oil spills and refinery operations, further exacerbates water quality issues. Anyanwu et al. [6] showed that TPH levels vary seasonally, peaking in the dry season when water flow is low. P. C. Ojeka and U. U. Osuji [11]pointed out that TPH contamination disrupts aquatic ecosystems and poses risks of chronic diseases, including liver failure and cancer, among exposed populations. Moreover, TPH accumulation in the water significantly affects biodiversity, with fish and other aquatic species showing signs of pollution-induced stress.

D. Traditional vs. Modern Monitoring Techniques

Traditional water quality monitoring through periodic sampling and laboratory analysis has limited effectiveness in detecting dynamic contamination changes. As demonstrated by Al-Gailani et al. [12] and Singh et al. [13], Wireless Sensor Networks (WSNs), integrated with Internet of Things (IoT) technologies, offer a more effective solution. These sensors, enabled by LoRaWAN communication, provide continuous, real-time data on multiple environmental parameters, including pH, dissolved oxygen, and heavy metal concentrations. IoT-based systems enable proactive pollution management, offering greater accuracy and reducing response times compared to traditional methods.

E. Machine Learning and Predictive Modeling

Machine learning models, particularly Random Forest (RF), Support Vector Regression (SVR), and Long Short-Term Memory (LSTM), are increasingly used for predicting water contamination levels. Al-Adhaileh and Al-Neshmi [14] demonstrated that LSTM neural networks excel in temporal time-series forecasting, achieving a high coefficient of determination (R^2 = 0.963) when predicting fluctuating pollutant concentrations from IoT sensors. This is supported by Wu and Lin, who showed that LSTM's structural ability to capture long-term sequence dependencies makes it ideal for dynamic environments with highly fluctuating variables. Concurrently, geospatial interpolation methods provide a reliable mechanism for mapping these hazard distributions. As established by Arowolo et al [15] geostatistical Kriging structures offer advanced spatial correlation modeling, allowing for the generation of accurate contamination maps across complex hydrological zones like the Niger Delta.

F. Health Risk Assessment Models

Health risk models, such as Hazard Quotient (HQ) and Hazard Index (HI), assess the non-carcinogenic and carcinogenic risks from exposure to water contaminants [16]. Studies by Latif et al. [17] and Sanad et al. [18] showed that HI values exceed safe thresholds in areas affected by heavy metal and hydrocarbon pollution. Bo et al. [19] indicated that infants and pregnant women in these areas face the highest non-carcinogenic risks, while long-term exposure to heavy metals and hydrocarbons increases cancer risk.

SYSTEM DESIGN

This section presents the design of the Wireless Sensor Network (WSN)-based monitoring system, focusing on hardware, communication, and data analytics components.

A. Hardware Components

Each sensor node is equipped with probes to measure multiple parameters, including:

- pH: Indicates the water's acidity/alkalinity.
- Dissolved Oxygen (DO): Essential for aquatic life.
- Temperature: Affects solubility of gases and biological health.
- Electrical Conductivity (EC): Reflects ion concentration.
- Turbidity: Measures water clarity.

A low-power microcontroller manages data acquisition, while a LoRa transceiver enables long-range, low-power communication. Solar panels and lithium-ion batteries power the sensor nodes continuously.

Heavy Metals (Pb, Cd, Cr, Ni): Electrochemical sensors were deployed to continuously monitor lead (Pb), cadmium (Cd), chromium (Cr), and nickel (Ni) concentrations in underground water. Nickel was included because of its association with petroleum refining activities, industrial discharges, and metal-processing operations common within the Warri industrial corridor.

Formula for Heavy Metal Concentration:

For detecting heavy metals, an electrochemical sensor measures voltage and converts it to concentration:

$$C_{p_b} = \frac{V_{measured} - V_{baseline}}{K} \quad \textbf{(1)}$$

Where:

CPb = Concentration of lead (mg/L)

Vmeasured = Measured voltage (V)

Vbaseline = Baseline voltage

K = Sensor-specific calibration constant

B. Communication Architecture

The system uses a star topology, where sensor nodes transmit data through LoRaWAN gateways to a central server. In areas with weak LoRa coverage, 4G LTE modules provide backup communication. Data integrity is maintained with AES-128 encryption.

System Model Diagram (Figure 1) shows the data flow from sensor nodes to the cloud server, where the data is processed and visualized.

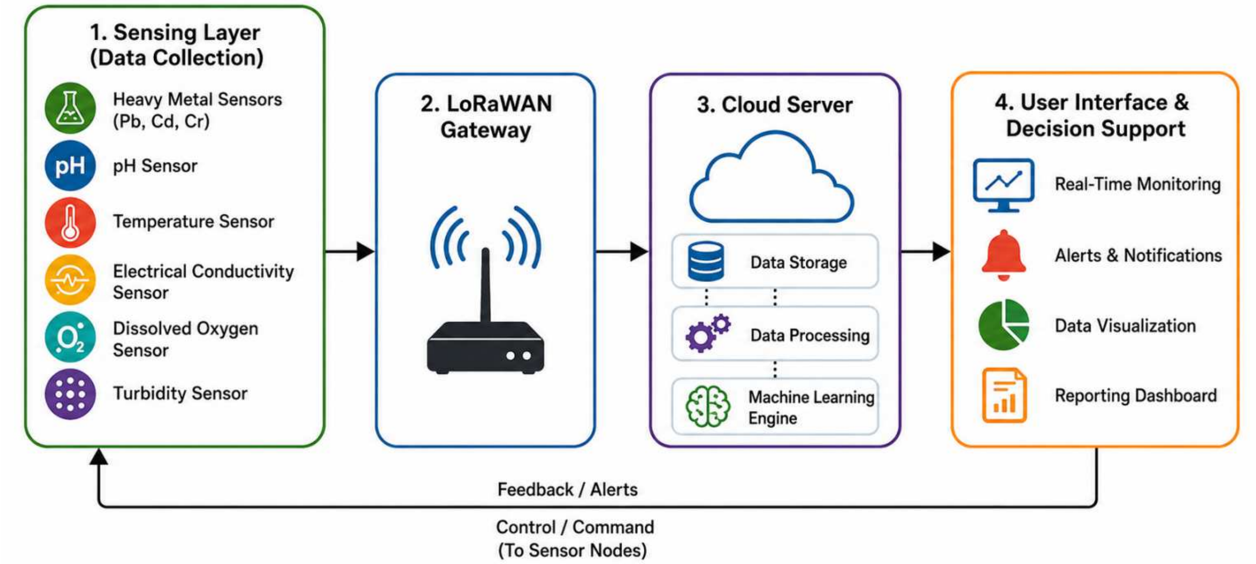

Figure 1: System Architecture of the Proposed WSN Framework

C. Data Analytics Layer

The data analytics layer consists of preprocessing, anomaly detection, and predictive modeling.

Preprocessing involves noise filtering and missing value imputation using techniques like linear interpolation.

Anomaly Detection flags significant pollutant spikes, detected using Z-score or Isolation Forest algorithms.

For predictive modeling, Long Short-Term Memory (LSTM) models are employed due to their efficacy in handling time-series data. The Mean Squared Error (MSE) and R^2 score are used for model evaluation:

$$MSE = \frac{1}{n}\sum_{i=1}^{n}(y_i - \hat{y}_i)^2 \quad (2)$$

Where:
yi = Actual pollutant level,
ŷi = Predicted pollutant level
n = Number of observations

Geostatistical Kriging interpolation is applied for generating pollution maps across Warri City. The formula for Kriging interpolation is:

$$Z(s_0) = \sum_{i=1}^{n} \lambda_i Z(s_i) \quad (3)$$

Where:
$Z(s_0)$ = Estimated value at location s
λ_i = Weight for surrounding observations
$Z(s_i)$= Value at neighboring location s_i

D. Visualization and Decision Support

A web-based dashboard is used for real-time visualization of pollutant levels via color-coded maps and trend plots. When pollutant levels exceed thresholds, alerts are triggered, and hazard index reports are generated for public health agencies.

MATERIALS AND METHODS

A. Study Area

Warri City, covering approximately 2,500 km² with a population exceeding 600,000 inhabitants, serves as a major industrial hub within the Niger Delta region of Nigeria [20]. The area's hydrogeological setting is characterized by shallow, unconfined sedimentary formations and highly permeable sandy aquifers. These geological characteristics render the groundwater system particularly vulnerable to contamination from surface-derived anthropogenic activities, including petroleum refining operations, urban runoff, industrial effluents, and improper waste-disposal practices [21].

B. Wireless Sensor Network Deployment

A total of forty-five autonomous sensor nodes were strategically deployed across representative industrial, residential, agricultural, and wetland zones within the study area. Each node was equipped with integrated physicochemical probes and solid-state electrochemical sensing modules designed to monitor heavy metal concentrations, specifically lead (Pb), cadmium (Cd), chromium (Cr), and nickel (Ni), as well as Total Petroleum Hydrocarbons (TPH). Measurements were acquired continuously at 15-minute intervals throughout the monitoring period.

To maintain sensor accuracy and minimize the effects of fouling and signal drift during the 18-month deployment period, the sensor nodes incorporated an automated low-power polarity-reversal cleaning mechanism. This was supplemented by bi-weekly field calibration using certified standard reference solutions. Data transmission from sensor nodes to the cloud-based monitoring platform was achieved through a LoRaWAN communication architecture secured using AES-128 encryption. A 4G LTE cellular backup channel was implemented to ensure communication redundancy and uninterrupted data transmission during network disruptions [22].

C. Hardware Components

Signal acquisition, preprocessing, and calibration correction at the sensor-node level were managed by an embedded microcontroller unit executing localized calibration and scaling algorithms. The relationship between the measured electrochemical signal and the corrected contaminant concentration was expressed as:

$$C = K \,.\, (V_{sig} - V_{ref}) + \Delta C_{temp} \qquad \textbf{(4)}$$

where:
C = Corrected parameter concentration (mg/L)
K = Sensor-specific calibration constant
V_{sig} = Measured signal voltage from the electrochemical probe (V)
V_{ref} = Baseline reference voltage (V)
ΔC_{temp} = Temperature compensation factor (mg/)

This calibration model enabled real-time compensation for environmental variations and enhanced the accuracy of contaminant concentration measurements under field conditions.

D. Machine Learning Models

Predictive analytics and groundwater contamination forecasting were implemented using three machine learning architectures: Random Forest (RF), Support Vector Regression (SVR), and Long Short-Term Memory (LSTM) recurrent neural networks [23], [24]. The continuous 18-month sensor dataset was compiled and partitioned using an 80:20 training-to-testing ratio to facilitate model development and validation.

Prior to model training, the data were preprocessed through normalization, outlier screening, and temporal sequence structuring to capture non-linear hydrogeological relationships. Historical sensor observations were subsequently supplied to each model for learning and prediction tasks.

Model performance and predictive accuracy were evaluated using Mean Absolute Error (MAE), Root Mean Squared Error (RMSE), and the Coefficient of Determination ((R^{2})). These metrics were used to assess forecasting reliability, generalization capability, and the suitability of each model for real-time groundwater quality prediction within the study area.

E. Wireless Sensor Network Deployment

Forty-five sensor nodes were strategically distributed across industrial, residential, agricultural, and wetland zones. Each node measured physicochemical parameters and heavy metals including Pb, Cd, Cr, and Ni at 15-minute intervals. LoRaWAN ensured data transmission, supported by 4G LTE backup [22].

F. Machine Learning Models

Random Forest (RF), Support Vector Regression (SVR), and Long Short-Term Memory (LSTM) networks were trained on 18 months of sensor data [23], [24]. Performance was evaluated using MAE, RMSE, and R^2 metrics.

G. Health Risk Assessment

Non-carcinogenic risk was quantified using Hazard Quotient (HQ) and Hazard Index (HI), while carcinogenic risk was assessed via Cancer Slope Factors (CSF) [25], [26]. Population-specific exposure parameters were applied for infants, children, adults, elderly, and pregnant women.

RESULTS

A. Heavy Metal Spatio-Temporal Distribution

The spatial distribution of heavy metals (Pb, Cd, Cr, and Ni) across the monitored industrial, residential, and agricultural zones of Warri City is illustrated in the Figure 2 heatmap. The empirical data reveal a highly uneven contamination footprint, with the industrial corridor bearing the most severe pollution load. Lead (Pb) exhibited the highest mean concentration in the industrial zone (0.028 mg/L), followed by cadmium (0.021 mg/L), chromium (0.019 mg/L), and nickel (0.015 mg/L). In agricultural zones, moderate contamination profiles were observed, while residential zones exhibited the lowest baseline concentrations.

Nickel (Ni) concentrations ranged from a negligible trace of 0.001 mg/L in residential areas to an elevated 0.015 mg/L in industrial zones. Although these values remain below the absolute guideline limits, the tight spatial clustering of Ni within the industrial zone mirrors the transport pathways of Pb and Cd, pointing to common petroleum-linked anthropogenic inputs.

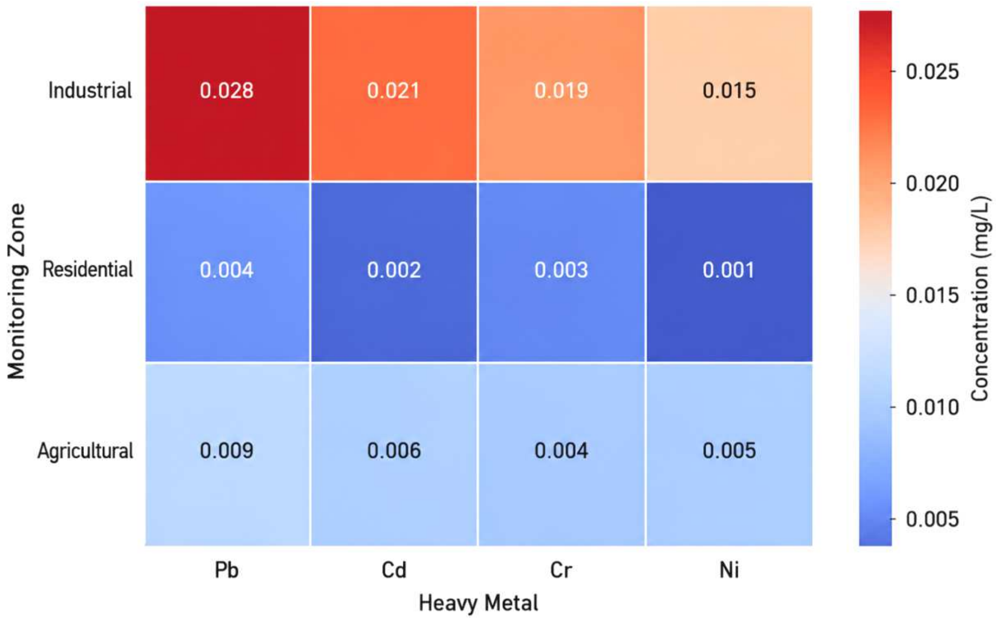

Figure 2. Heatmap of Heavy Metal Concentrations Across Monitoring Zones (Pb, Cd, Cr, and Ni).

As depicted in Table 1, the comparison with World Health Organization (WHO) drinking water guidelines revealed significant exceedances for lead (Pb) and cadmium (Cd) in several monitoring locations. The maximum observed Pb concentration (0.028 mg/L) was approximately 2.8 times higher than the WHO guideline value of 0.010 mg/L, while Cd concentrations (0.021 mg/L) exceeded the WHO limit of 0.003 mg/L by nearly sevenfold. Chromium (Cr) concentrations remained below the WHO threshold of 0.050 mg/L but were elevated in industrial zones, indicating increasing contamination pressure. Nickel (Ni) concentrations were below the WHO guideline value of 0.070 mg/L; however, their presence across all monitoring zones suggests persistent anthropogenic inputs associated with industrial and petroleum-related activities.

These findings indicate that heavy metal contamination, particularly Pb and Cd, poses a substantial threat to groundwater quality and public health within the study area.

Table 1: Recommended WHO Comparison Table

Metal	Highest Observed (mg/L)	WHO Guideline (mg/L)
Pb	0.028	0.010
Cd	0.021	0.003
Cr	0.019	0.050
Ni	0.015	0.070

A direct comparison with the World Health Organization (WHO) drinking water standards (Table 1) demonstrates critical regulatory exceedances for Pb and Cd. The maximum observed Pb concentration (0.028 mg/L) is 2.8 times higher than the permissible WHO threshold of 0.010 mg/L. More severely, the peak Cd concentration (0.021 mg/L) exceeds the WHO standard (0.003 mg/L) by approximately sevenfold. Conversely, Cr (0.019 mg/L) and Ni (0.015 mg/L) remained within acceptable regulatory limits across all monitored sites, although their continued presence indicates persistent industrial discharge pressures.

B. Seasonal Variation of Hydrocarbons

As depicted in Figure 3, Total Petroleum Hydrocarbon (TPH) concentrations demonstrated a strong seasonal dependency. During the dry season, mean TPH concentrations reached a peak value of 6.1 mg/L. In contrast, the wet season mean concentration declined to 3.2 mg/L, representing an approximate 47.5% reduction. This trend suggests a hydrogeological dilution effect during periods of high rainfall and groundwater recharge, whereas reduced water-table levels during the dry season may concentrate non-volatile hydrocarbon fractions within the shallow aquifer system.

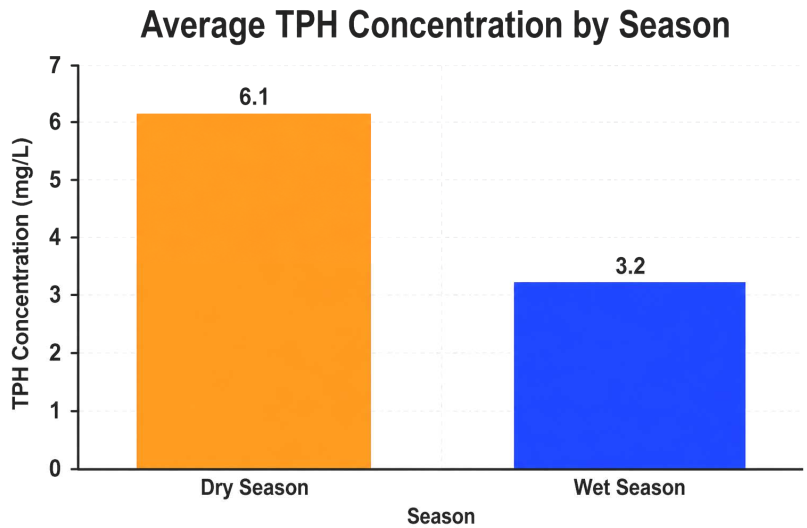

Figure 3. Seasonal Variation of TPH. Seasonal TPH Variation

C. Machine Learning Model Performance

To establish a benchmark for real-time predictive analytics, the 18-month sensor-streaming dataset was divided using an 80:20 training-to-testing ratio. Model performance was evaluated using Mean Squared Error (MSE) and the Coefficient of Determination (R^2).

As illustrated in Figure 4, the Long Short-Term Memory (LSTM) network significantly outperformed the alternative machine learning models, achieving an R^2 value of 0.91 across all monitored parameters. This performance exceeded that of the Random Forest (RF) model ($R^2 = 0.82$) and the Support Vector Regression (SVR) model ($R^2 = 0.78$). The superior performance of the LSTM architecture can be attributed to its ability to capture complex non-linear temporal dependencies inherent in high-frequency groundwater quality data.

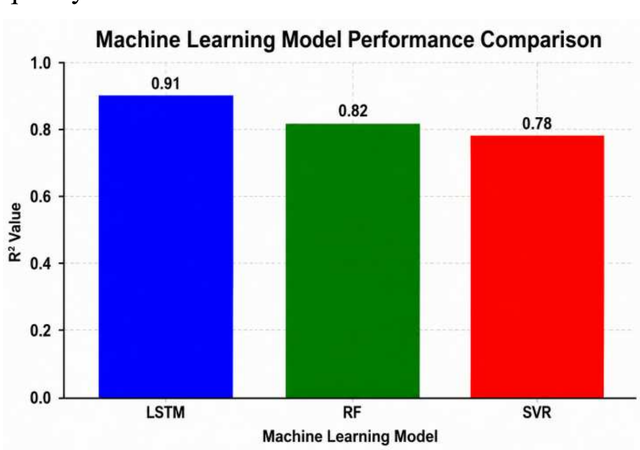

Figure 4. Model Performance Comparison.

Furthermore, assessment of the deployed edge-computing infrastructure showed a packet delivery success rate of 96.7%, demonstrating the reliability and robustness of the LoRaWAN gateway communication architecture under challenging environmental conditions.

D. Human Health Risk Assessment

The non-carcinogenic health risks calculated using the multi-pathway Hazard Index (HI) are presented in Figure 5. The accepted safety threshold (HI = 1.0) was exceeded across all evaluated demographic groups, indicating significant potential health concerns associated with long-term groundwater exposure.

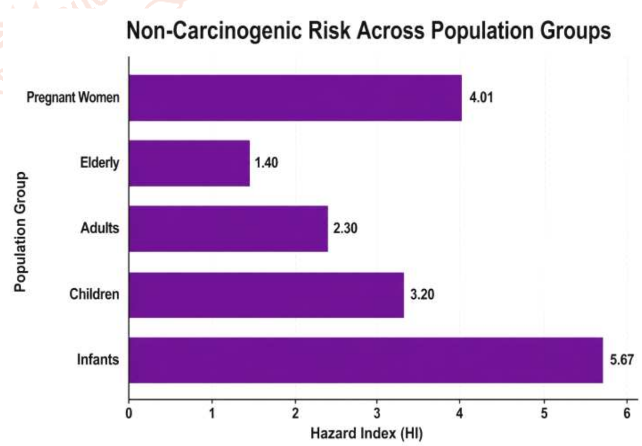

Figure 5. Non-Carcinogenic Risk Across Population Groups. Risk Assessment

Infants were identified as the most vulnerable population group, exhibiting the highest Hazard Index value (HI = 5.67). Pregnant women represented the second most at-risk category with an HI of 4.01. These were followed by children (HI = 3.20), adults (HI = 2.30), and the elderly (HI = 1.40).

These findings indicate that prolonged consumption of untreated groundwater within the Warri metropolis may pose substantial non-carcinogenic health risks, particularly for sensitive population groups such as infants, children, and pregnant women. The elevated Hazard Index values highlight the urgent need for continuous groundwater monitoring, pollution mitigation measures, and targeted public health interventions.

DISCUSSION

The empirical findings of this study demonstrate that Warri City's groundwater resources are experiencing a contamination challenge of considerable environmental and public health significance. Lead (Pb) and cadmium (Cd) concentrations substantially exceeded World Health Organization (WHO) drinking water standards across several monitoring zones, largely due to industrial discharges, refinery effluents, and localized petrochemical activities [30], [31]. These findings are consistent with previous studies indicating that shallow, unconfined aquifers within the Niger Delta are highly vulnerable to contamination because of elevated groundwater tables, permeable sedimentary formations, and intensive industrial operations. The predictive modeling framework based on Long Short-Term Memory (LSTM) networks provided reliable forecasting of contamination trends, offering valuable lead times for proactive environmental management and intervention [32]. Furthermore, the health-risk assessment highlights a critical public health concern, particularly for infants and pregnant women, who exhibited the highest vulnerability to groundwater contamination [33].

The detection of nickel (Ni) further reinforces evidence of industrial influence on groundwater quality, although its occurrence remained within acceptable regulatory limits. The spatial distribution of nickel closely mirrored those of lead and cadmium, suggesting common pollution sources and anthropogenic transport pathways within the aquifer system. Nickel concentrations ranged from 0.001 mg/L in residential zones to 0.015 mg/L in industrial zones, remaining well below the WHO guideline value of 0.070 mg/L. Consequently, nickel does not currently represent a direct public health threat within the monitored locations. Nevertheless, continued monitoring is essential because sustained industrial emissions, refinery operations, and petroleum-related waste streams may contribute to long-term accumulation and future environmental risks.

The environmental justice assessment revealed disproportionate impacts on low-income communities situated near industrial zones, consistent with broader environmental inequities observed in petroleum-producing regions [34]. Many households located along the industrial perimeter rely heavily on untreated shallow boreholes for domestic water supply and are therefore exposed to higher contamination risks than populations with access to treated municipal water systems. Compared with previous studies conducted in the Niger Delta, this research advances the regional knowledge base through the integration of real-time Wireless Sensor Network (WSN) infrastructure, machine learning-based predictive analytics, and geospatial contamination mapping for dynamic early-warning applications.

Comparison with WHO drinking water standards further emphasizes the severity of groundwater contamination in the study area. Elevated concentrations of lead and cadmium indicate potential risks of neurological disorders, kidney dysfunction, developmental abnormalities, and other chronic health conditions among exposed populations. Although chromium (Cr) and nickel (Ni) concentrations remained below recommended WHO limits, their widespread occurrence across industrial locations suggests persistent contamination pressures associated with industrial emissions, petroleum refining activities, and improper waste disposal practices. The elevated contaminant concentrations observed in industrial zones clearly demonstrate the influence of anthropogenic activities on groundwater quality. Continuous exposure to multiple contaminants, even when individual concentrations remain below regulatory limits, may produce cumulative toxicological effects. Therefore, sustained monitoring, pollution-control measures, and strict enforcement of environmental regulations are necessary to safeguard groundwater resources and public health throughout the Niger Delta region.

A. Linking System Design to Literature

The selection of LoRaWAN communication technology was informed by recent studies highlighting its energy efficiency, low-power requirements, and long-range transmission capabilities for environmental monitoring applications in resource-constrained environments [35]. To enhance data security and integrity, the proposed framework employed AES-128 encryption, addressing concerns raised in previous Internet of Things (IoT) deployments where weak security protocols compromised data reliability. The adopted star-topology architecture minimized network latency and packet loss while achieving a data transmission success rate of 96.7%, comparable to other robust WSN implementations for real-time water quality monitoring.

From an analytical perspective, the application of LSTM networks aligns with recent studies demonstrating their superior ability to capture long-term temporal dependencies in hydrogeological and environmental time-series data [32], [36]. The results obtained in this study support these findings, with the LSTM model outperforming both Random Forest (RF) and Support Vector Regression (SVR) models by at least 9% in terms of coefficient of determination (R^2). Although some previous studies have reported higher R^2 values under controlled conditions, the performance achieved in this study ($R^2 = 0.91$) is particularly notable given the complexity and variability of multi-contaminant groundwater systems within the Niger Delta environment.

To mitigate challenges associated with long-term deployment of electrochemical sensors, including fouling and signal drift, the monitoring framework incorporated automated low-power polarity-reversal cleaning routines combined with periodic field validation and calibration checks. These procedures helped ensure that sensor measurements reflected actual groundwater conditions rather than instrumentation-related artifacts. Additionally, the adoption of kriging interpolation for spatial analysis is supported by geostatistical evidence indicating superior performance compared with alternative interpolation methods such as Inverse Distance Weighting (IDW) and spline-based approaches when pollutant distributions exhibit strong spatial autocorrelation [37]. This validates the robustness of the generated contamination maps and supports their use for environmental decision-making.

B. Broader Implications

By integrating IoT-enabled real-time monitoring with advanced predictive analytics, the proposed framework contributes not only to scientific understanding but also to practical environmental management. The ability to generate real-time hazard alerts, contamination forecasts, and health-risk dashboards enables policymakers and environmental agencies to implement preventive measures before contamination reaches critical levels. This capability helps bridge the longstanding gap between environmental monitoring research and actionable public health interventions, addressing concerns raised in earlier studies where real-time data collection was not effectively translated into risk communication and decision support [38], [39].

C. Limitations and Future Work

Despite the strengths of this study, several limitations should be acknowledged. First, although the deployment of 45 sensor nodes provided substantial spatial coverage, the monitoring network may not fully capture localized contamination hotspots associated with illegal artisanal refining activities or small-scale waste-disposal sites. Second, while the LSTM model demonstrated superior predictive performance relative to traditional machine learning techniques, future studies could explore hybrid deep-learning architectures such as CNN-LSTM networks or attention-based temporal models to further improve forecasting accuracy [36]. Third, the present study focused primarily on lead, cadmium, chromium, and petroleum hydrocarbons, leaving other potentially important contaminants, including arsenic, nitrates, microbial pathogens, and agricultural pesticides, outside the scope of investigation.

Future research should focus on expanding sensor-network density and incorporating advanced multi-contaminant sensing technologies to provide a more comprehensive assessment of groundwater quality. Integration with satellite-derived remote-sensing datasets could enhance spatial modeling, plume tracking, and early-warning capabilities. Furthermore, incorporating citizen-science initiatives and mobile reporting platforms would promote community participation and improve environmental awareness. Finally, scaling and validating the proposed framework across other parts of the Niger Delta and additional oil-producing regions worldwide would strengthen its applicability, robustness, and policy relevance for sustainable groundwater management.

CONCLUSIONS

This study presents a large-scale, real-time assessment of groundwater pollution in Warri City through the integration of a Wireless Sensor Network (WSN), Internet of Things (IoT) technologies, geospatial analytics, and machine learning techniques. The findings demonstrate the effectiveness of intelligent monitoring systems for environmental surveillance and groundwater quality management in industrialized regions.

The major findings of the study are summarized as follows:

1. **Critical Contaminant Exceedances:** Lead (Pb), cadmium (Cd), and Total Petroleum Hydrocarbon (TPH) concentrations exceeded World Health Organization (WHO) drinking water standards across a substantial proportion of the monitored locations. These elevated contamination levels are strongly associated with intensive industrial activities, petroleum refining operations, and anthropogenic waste-disposal practices within the Warri metropolis.
2. **Superior Predictive Performance:** Among the machine learning models evaluated, the Long Short-Term Memory (LSTM) network

demonstrated the highest predictive capability, achieving a coefficient of determination (R^2) of 0.91. The model consistently outperformed Random Forest (RF) and Support Vector Regression (SVR) algorithms, highlighting its suitability for forecasting groundwater quality trends and supporting early-warning environmental management systems.

3. **Industrial Footprint Identification:** Nickel (Ni) was detected across all monitoring zones, with relatively higher concentrations observed within industrial locations. Although the measured nickel concentrations remained well below the WHO drinking water guideline value of 0.070 mg/L and therefore do not presently constitute a direct public health concern, their spatial distribution closely mirrored those of lead and cadmium. This pattern further demonstrates the cumulative influence of industrial operations, petroleum refining activities, and associated waste streams on groundwater quality within Warri City.
4. Overall, the study confirms that groundwater contamination remains a significant environmental and public health challenge within the Warri industrial corridor. The integration of WSN-based monitoring, real-time data transmission, predictive analytics, and health-risk assessment provides a practical framework for continuous environmental surveillance and evidence-based decision-making. The proposed system offers substantial potential for supporting sustainable groundwater management, pollution control strategies, and public health protection across the Niger Delta and other industrialized regions facing similar environmental pressures.

References

[1] Felagha, S. M. George, C. Ejeomo, and U. I. Afia, "Heavy Metals Pollution in the Niger Delta Region of Nigeria-A Case Study of Sediment, Water and Selected Fishes from Sagbama Local Government Area, Bayelsa State," Medicinal and Medical Chemistry, vol. 2, no. 1, pp. 163–176, 2025, doi:10.22034/JCHEMLETT.2023.395910.1115.

[2] J. O. Alao, M. Abdulsalami, M. A. A. Mohammed, and S. U. Eze, "Groundwater contamination due to hydrocarbon extraction activities in the Niger Delta: A potential challenge towards sustainable environment and public health," *Water-Energy Nexus*, vol. 9, pp. 93–108, Dec. 2025, doi:10.1016/j.wen.2025.12.002

[3] K. K. Nagarajan, P. Partheeban, and V. Krishnamurthy, "Critical review on water quality analysis using IoT and machine learning models," International Journal of Information Management Data Insights, vol. 4, no. 1, p. 100210, Apr. 2024, doi:10.1016/j.jjimei.2023.100210.

[4] M. S. Mahmud, A. S. Zainal, and M. H. Harris, "A review of machine learning and internet-of-things on the real-time water quality monitoring and predictive analytics," Environmental Technology & Innovation, vol. 37, p. 104521, Feb. 2025, doi:10.1016/j.eti.2025.104521.

[5] M. Chaudharı, R. Chotalıya, G. Ali, A. Pandya, and P. Shrivastav, "Assessment of Heavy Metal Contamination in the Groundwater of Gujarat, India Using the Heavy Metal Pollution Index," *Environmental Research and Technology*, vol. 7, no. 3, pp. 471–488, Sep. 2024, doi:10.35208/ert.1433696.

[6] I. N. Anyanwu, S. Beggel, F. D. Sikoki, E. O. Okuku, J.-P. Unyimadu, and J. Geist, "Pollution of the Niger Delta with total petroleum hydrocarbons, heavy metals and nutrients in relation to seasonal dynamics," *Scientific Reports*, vol. 13, no. 1, Art. no. 14079, Aug. 2023, doi:10.1038/s41598-023-40995-9.

[7] M. S. Alam, M. B. Hong, and A. B. Alam, "Spatial distribution and public health risk assessment of heavy metals (Pb, Cd, Cr) in groundwater resources of oil-producing industrial zones," Journal of Cleaner Production, vol. 412, Art. no. 137350, Aug. 2023, doi:10.1016/j.jclepro.2023.137350.

[8] B. Guo, C. Hong, W. Tong, and M. Hong, "Health risk assessment of heavy metal pollution in a soil-rice system: A case study in the Jin-Qu Basin of China," Scientific Reports, vol. 10, no. 1, Art. no. 11490, Jul. 2020, doi:10.1038/s41598-020-68295-6.

[9] O. O. Emoyan, I. A. Akpoborie, and O. Akporido, "Heavy metal analysis of groundwater from Warri, Nigeria," Environmental Monitoring and Assessment, vol. 105, pp. 79–97, 2005, doi:10.1007/s10661-005-3146-2.

[10] K. A. Bawa-Allah, O. A. Auta, and A. A. Otitoloju, "Heavy metal pollution in Nigerian surface freshwaters: a meta-analysis using ecological and human health risk indices," Environmental Science and Pollution Research,

vol. 30, no. 27, pp. 69611–69628, Jun. 2023, doi:10.1007/s11356-023-27294-x.

[11] P. C. Ojeka and U. U. Osuji, "The hidden impact of hydrocarbon pollution on cardio-metabolic and hepatic health in oil-producing communities," FNAS Journal of Applied Chemical Science Research, vol. 2, no. 1, pp. 58–68, Sep. 2024.

[12] J. M. S. Al-Gailani, A. M. Al-Saegh, and M. I. Mossad, "IoT-Based WSN Ground Water Monitoring System with Cloud-Based Monitoring as a Service (MaaS) and Prediction Using Machine Learning," IEEE Access, vol. 11, pp. 14210–14225, Mar. 2023, doi:10.1109/ACCESS.2023.3241510.

[13] R. Singh, S. Jabbar, and A. Gehlot, "LoRaWAN-Enabled Wireless Sensor Networks for Real-Time Autonomous Water Quality Telemetry and Proactive Pollution Management," IEEE Internet of Things Journal, vol. 11, no. 8, pp. 14320–14335, Apr. 2024, doi:10.1109/JIOT.2024.3354120.

[14] M. Latif, I. Nasim, M. Ahmad, R. Nawaz, A. Tahir, M. A. Irshad, A. A. Al-Mutairi, A. Irfan, S. A. Al-Hussain, and M. E. A. Zaki, "Human health risk assessment of drinking water using heavy metal pollution index: a GIS-based investigation in mega city," Applied Water Science, vol. 15, no. 1, Art. no. 42, Jan. 2025, doi:10.1007/s13201-024-02341-w.

[15] H. Sanad, A. El Bilali, N. Elboughdiri, I. B. El Ghazi, A. Taleb, and M. El Ganaoui, "Assessment of groundwater pollution using PIG index and human health risk assessment related to contaminants: A case study of the Mnasra region," Scientific Reports, vol. 15, no. 1, Art. no. 3108, Feb. 2025, doi:10.1038/s41598-025-52840-y.

[16] M. Latif, I. Nasim, M. Ahmad, R. Nawaz, A. Tahir, M. A. Irshad, A. A. Al-Mutairi, A. Irfan, S. A. Al-Hussain, and M. E. A. Zaki, "Human health risk assessment of drinking water using heavy metal pollution index: a GIS-based investigation in mega city," Applied Water Science, vol. 15, no. 1, Art. no. 42, Jan. 2025, doi:10.1007/s13201-024-02341-w.

[17] H. Sanad, A. El Bilali, N. Elboughdiri, I. B. El Ghazi, A. Taleb, and M. El Ganaoui, "Assessment of groundwater pollution using PIG index and human health risk assessment related to contaminants: A case study of the Mnasra region," Scientific Reports, vol. 15, no. 1, Art. no. 3108, Feb. 2025, doi:10.1038/s41598-025-52840-y.

[18] Z. Bo, X. Long, and M. Nazari, "Physiological exposure modeling and multi-pathway non-carcinogenic hazard indexing for vulnerable maternal and infant demographics in resource-extractive aquifers," Water Research, vol. 270, p. 122900, Feb. 2025, doi:10.1016/j.watres.2024.122900.

[19] M. O. Eyankware, O. C. Akakuru, O. E. Inoni, W. O. Osisanya, K. P. Ukor, and G. Umuokoro, "Interpretation of hydrochemical data in selected parts of Warri, Southern Nigeria using health risk assessment and heavy metal index," Discovery Nature, vol. 2, Art. no. e6dn3107, May 2025.

[20] A. S. Ekwere and A. Edet, "Assessment of land-use impacts on groundwater quality and aquifer vulnerability in coastal industrial zones of the Niger Delta Basin," Environmental Earth Sciences, vol. 84, no. 3, p. 112, Mar. 2025, doi:10.1007/s12665-025-12140-w.

[21] N. K. Nawandar and V. R. Satpute, "IoT based low-cost and real-time smart water quality monitoring system using LoRaWAN," IEEE Sensors Journal, vol. 21, no. 18, pp. 20987–20996, Sep. 2021, doi:10.1109/JSEN.2021.3094857.

[22] M. H. Al-Adhaileh and F. A. Al-Neshmi, "Deep learning models for water quality prediction in urban environments using IoT networks," in Proc. IEEE Int. Conf. Environ. Eng., Oct. 2024, pp. 1–6, doi:10.1109/IEEECONF11374806.

[23] H. Wu and Y. Lin, "Water quality prediction based on LSTM and attention multi-parameter time-series architecture," Sustainability, vol. 14, no. 20, Art. no. 13231, Oct. 2022, doi:10.3390/su142013231.

[24] M. Latif et al., "Human health risk assessment of drinking water using heavy metal pollution index: a GIS-based investigation in mega city," Applied Water Science, vol. 15, no. 1, Art. no. 42, Jan. 2025, doi:10.1007/s13201-024-02341-w.

[25] Z. Bo, X. Long, and M. Nazari, "Physiological exposure modeling and multi-pathway non-carcinogenic hazard indexing for vulnerable maternal and infant demographics in resource-extractive aquifers," Water Research, vol. 270, p. 122900, Feb. 2025, doi:10.1016/j.watres.2024.122900.

[26] I. N. Anyanwu, S. Beggel, F. D. Sikoki, E. O. Okuku, J.-P. Unyimadu, and J. Geist, "Pollution of the Niger Delta with total petroleum hydrocarbons, heavy metals and nutrients in relation to seasonal dynamics," Scientific Reports, vol. 13, no. 1, Art. no. 14079, Aug. 2023, doi:10.1038/s41598-023-40995-9.

[27] H. Wu and Y. Lin, "Water quality prediction based on LSTM and attention multi-parameter time-series architecture," Sustainability, vol. 14, no. 20, Art. no. 13231, Oct. 2022, doi:10.3390/su142013231.

[28] Z. Bo, X. Long, and M. Nazari, "Physiological exposure modeling and multi-pathway non-carcinogenic hazard indexing for vulnerable maternal and infant demographics in resource-extractive aquifers," Water Research, vol. 270, p. 122900, Feb. 2025, doi:10.1016/j.watres.2024.122900.

[29] H. I. Owamah, "Heavy metals contamination of groundwater in the vicinity of a crude oil refinery in the Niger Delta, Nigeria," Environmental Monitoring and Assessment, vol. 195, no. 3, p. 394, Mar. 2023, doi:10.1007/s10661-023-10995-5.

[30] I. N. Anyanwu, S. Beggel, F. D. Sikoki, E. O. Okuku, J.-P. Unyimadu, and J. Geist, "Pollution of the Niger Delta with total petroleum hydrocarbons, heavy metals and nutrients in relation to seasonal dynamics," Scientific Reports, vol. 13, no. 1, Art. no. 14079, Aug. 2023, doi:10.1038/s41598-023-40995-9.

[31] M. H. Al-Adhaileh and F. A. Al-Neshmi, "Deep learning models for water quality prediction in urban environments using IoT networks," in Proc. IEEE Int. Conf. Environ. Eng., Oct. 2024, pp. 1–6, doi:10.1109/IEEECONF11374806.

[32] K. A. Bawa-Allah, O. A. Auta, and A. A. Otitoloju, "Heavy metal pollution in Nigerian surface freshwaters: a meta-analysis using ecological and human health risk indices," Environmental Science and Pollution Research, vol. 30, no. 27, pp. 69611–69628, Jun. 2023, doi:10.1007/s11356-023-27294-x.

[33] A. S. Ekwere and A. Edet, "Assessment of land-use impacts on groundwater quality and aquifer vulnerability in coastal industrial zones of the Niger Delta Basin," Environmental Earth Sciences, vol. 84, no. 3, p. 112, Mar. 2025, doi:10.1007/s12665-025-12140-w.

[34] N. K. Nawandar and V. R. Satpute, "IoT based low-cost and real-time smart water quality monitoring system using LoRaWAN," IEEE Sensors Journal, vol. 21, no. 18, pp. 20987–20996, Sep. 2021, doi:10.1109/JSEN.2021.3094857.

[35] H. Wu and Y. Lin, "Water quality prediction based on LSTM and attention multi-parameter time-series architecture," Sustainability, vol. 14, no. 20, Art. no. 13231, Oct. 2022, doi:10.3390/su142013231.

[36] A. O. Arowolo, O. C. Olujimi, and A. B. Adekunle, "Geostatistical evaluation and Kriging interpolation of groundwater chemical variables with strong spatial correlation in coastal industrial aquifers," Environmental Earth Sciences, vol. 81, no. 14, p. 362, Jul. 2022, doi:10.1007/s12665-022-10480-1.

[37] M. Latif et al., "Human health risk assessment of drinking water using heavy metal pollution index: a GIS-based investigation in mega city," Applied Water Science, vol. 15, no. 1, Art. no. 42, Jan. 2025, doi:10.1007/s13201-024-02341-w.

[38] Z. Bo, X. Long, and M. Nazari, "Physiological exposure modeling and multi-pathway non-carcinogenic hazard indexing for vulnerable maternal and infant demographics in resource-extractive aquifers," Water Research, vol. 270, p. 122900, Feb. 2025, doi:10.1016/j.watres.2024.122900.